

# Unconventional superconductivity and anomalous response in hole-doped transition metal dichalcogenides

Evan Sosenko,<sup>\*</sup> Junhua Zhang,<sup>†</sup> and Vivek Aji<sup>‡</sup>*Department of Physics, University of California, Riverside, Riverside, California 92521, USA*

(Received 6 December 2015; revised manuscript received 14 March 2017; published 18 April 2017)

Two-dimensional transition metal dichalcogenides entwine interaction, spin-orbit coupling, and topology. Hole-doped systems lack spin degeneracy: states are indexed with spin and valley specificity. This unique structure offers new possibilities for correlated phases and phenomena. We realize an unconventional superconducting pairing phase which is an equal mixture of a spin singlet and the  $m = 0$  spin triplet. It is stable against large in-plane magnetic fields, and its topology allows quasiparticle excitations of net nonzero Berry curvature via pair-breaking circularly polarized light.

DOI: [10.1103/PhysRevB.95.144508](https://doi.org/10.1103/PhysRevB.95.144508)

## I. INTRODUCTION

The interplay of spin-orbit interaction and electron-electron interaction is a fertile area of research where new phases of matter and novel phenomena have been theoretically conjectured and experimentally realized [1–7]. Single-layer transition metal group-VI dichalcogenides (TMDs),  $MX_2$  ( $M = \text{Mo, W}$  and  $X = \text{S, Se, and Te}$ ), are direct-band-gap semiconductors that have all the necessary ingredients to explore these phenomena [8–18]. While sharing the hexagonal crystal structure of graphene, they differ in three important aspects: (1) gapped valleys as opposed to Dirac nodes; (2) broken inversion symmetry and strong spin-orbit coupling yielding a large splitting of the valence bands; and (3) the bands near the chemical potential predominantly have the transition metal  $d$ -orbital character [19–24].

The inversion symmetry breaking and the strong spin-orbit coupling due to the heavy transition element (Mo and W) endow the bands with nontrivial Berry curvature. A remarkable consequence is that spin-preserving optical transitions between valence and conduction bands are allowed, even though the atomic orbitals involved all have a  $d$  character. Furthermore, the valley-dependent sign of the Berry curvature leads to selective photoexcitation: right circular polarization couples to one valley, and left circular polarization to the other. This enables a number of valleytronic and spintronic applications that have attracted a lot of attention over the last few years [25–27].

We are primarily interested in exploiting the band structure and valley-contrasting probe afforded by the nontrivial topology in order to study and manipulate correlated phenomena in these systems. In particular, we focus on hole-doped systems, where an experimentally accessible window in energy is characterized by two disconnected pieces of spin nondegenerate Fermi surfaces. One can preferentially excite electrons from either Fermi surface. Since the spins are locked to their valley index, these excitations have specific  $s_z$  (where

the  $z$  axis is perpendicular to the two-dimensional crystal). We focus on the possible superconducting states and their properties.

Spin-valley locking and its consequence for superconductivity, dubbed Ising superconductivity, has been previously studied for heavily doped  $p$ -type and  $n$ -type TMDs [28–32], where Fermi surfaces of each spin are present in each valley. Our focus is the regime of maximal loss of spin degeneracy where the effects are most striking [33]. The two valleys in the energy landscape generically allow two classes of superconducting phases: intervalley pairing with zero center of mass momentum, and intravalley pairing with finite Cooper pair center of mass. Since the center of symmetry is broken and spin degeneracy is lost, classifications of superconducting states by parity, i.e., singlet versus triplet, is no longer possible. In this paper, we study both extrinsic and intrinsic superconductivity by projecting the interactions and pairing potential to the topmost valence band. We identify the possible phases, and analyze the nature of the optoelectronic coupling and the response to magnetic fields. Our main conclusions are as follows:

(1) For both proximity to an  $s$ -wave superconductor, and due to local attractive density-density interactions, the leading instability is due to an intervalley paired state, where the Cooper pair is an equal mixture of a spin singlet and the  $m = 0$  spin triplet [34].

(2) While the valley selectivity of the optical transition is suppressed, it remains finite. Consequently, the two quasiparticles generated by pair-breaking circularly polarized light are correlated such that one is in the valence band of one valley and the conduction band of the other. The valley and bands are determined by the polarity of incident light.

(3) The quasiparticles generated in (2) both have the same charge and Berry curvature. Thus an anomalous Hall effect is anticipated as the two travel in the same direction transverse to an applied electric field.

(4) An in-plane magnetic field tilts the spin, modifying the internal structure of the Cooper pair, however, no pair-breaking is induced in the absence of scalar impurities. The suppression of the effective interaction leads to a parametric reduction of the transition temperature. In the presence of scalar impurities, pair-breaking is enabled, but the associated critical magnetic field is large.

<sup>\*</sup>evan.sosenko@email.ucr.edu; <https://evansosenko.com>

<sup>†</sup>junhua.zhang@ucr.edu

<sup>‡</sup>vivek.aji@ucr.edu

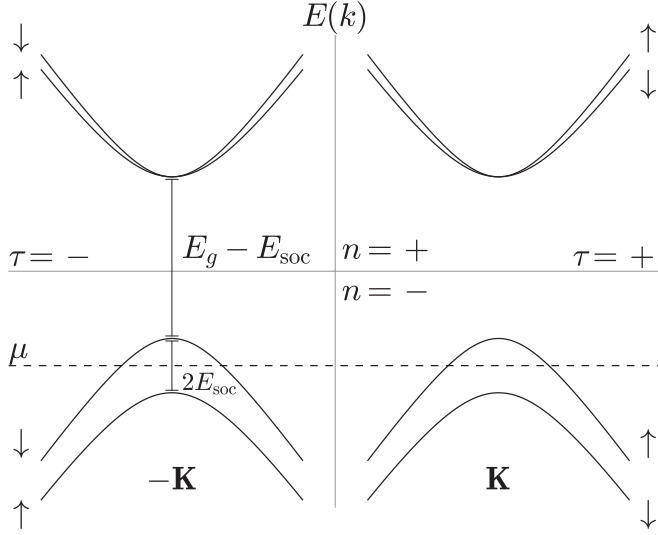


FIG. 1. Energy bands for WSe<sub>2</sub> as given by Eq. (2) with  $at = 3.939 \text{ eV \AA}^{-1}$ ,  $E_g = 1.60 \text{ eV}$ , and  $E_{\text{soc}} = 0.23 \text{ eV}$ . Each valley is centered at  $\pm\mathbf{K}$  relative to the center of the Brillouin zone. The energy for a given band depends only on the distance  $k$  measured from the valley center.

## II. MODEL

The TMD system is described by the effective tight-binding, low-energy, two-valley Hamiltonian [26],

$$H_{\tau}^0(\mathbf{k}) = at(\tau k_x \hat{\sigma}_x + k_y \hat{\sigma}_y) + \frac{E_g}{2} \hat{\sigma}_z - E_{\text{soc}} \tau \frac{\hat{\sigma}_z - 1}{2} \hat{s}_z, \quad (1)$$

where the Pauli matrices  $\hat{s}_i$  operate in the spin space and  $\hat{\sigma}_i$  operate in the orbital space with the two Bloch orbital states  $|v_{\tau s}^v(\mathbf{k})\rangle$  (indexed by  $v = +$  for the in-plane orbital state  $|d_{x^2-y^2}\rangle + i\tau|d_{xy}\rangle$  and  $v = -$  for the out-of-plane orbital state  $|d_z\rangle$ ),  $s = \pm$  is the spin index, and  $\tau = \pm$  is the valley index corresponding to the  $\pm\mathbf{K}$  point, respectively. The momentum  $\mathbf{k} = (k_x, k_y)$  is measured from the valley center,  $a$  is the lattice constant,  $t$  is the hopping parameter,  $E_g$  represents the energy gap between the conduction and valence bands, and  $2E_{\text{soc}}$  is the spin splitting energy in the valence bands due to spin-orbit interaction.

The energy spectrum

$$2E_{\tau s}^n(k) = \tau s E_{\text{soc}} + n \sqrt{(2atk)^2 + (E_g - \tau s E_{\text{soc}})^2} \quad (2)$$

with  $k = |\mathbf{k}|$  and  $n = 1$  ( $n = -1$ ) indexing the conduction (valence) band is shown in Fig. 1.

We focus on doped systems such that the chemical potential  $\mu$  lies in the upper valence bands. Within each band, the Bloch basis eigenstates are written in terms of the orbital states as elements on the Bloch sphere,

$$|u_{\tau s}^n(k, \phi)\rangle = \cos \frac{\theta_{\tau s}^n(k)}{2} |v_{\tau s}^+(k, \phi)\rangle + e^{-i\tau\phi} \sin \frac{\theta_{\tau s}^n(k)}{2} |v_{\tau s}^-(k, \phi)\rangle, \quad (3)$$

where  $k_x + i\tau k_y = ke^{i\tau\phi}$  and

$$\tan \frac{\theta_{\tau s}^n(k)}{2} = \frac{at\tau k}{\frac{E_g}{2} - E_{\tau s}^n(k)} = \frac{at\tau k}{E_{\tau s}^n(k) - E_{\tau s}^n(0)}. \quad (4)$$

The polar angle on the Bloch sphere of the conduction and valence bands are related by  $\theta_{\tau s}^-(k) - \theta_{\tau s}^+(k) = \tau\pi$ . The mapping of the energy band to the Bloch sphere, parametrized by  $(\theta, \phi)$ , encodes the topological character: as one moves from the node out to infinity, the states sweep either the northern or southern hemisphere with a chirality determined by the Berry curvature.

## III. SUPERCONDUCTIVITY

We consider two approaches to realizing a superconducting state. First, we assume a proximity induced state obtained by layering a TMD on an  $s$ -wave superconductor. Second, we study an intrinsic correlated phase arising from density-density interactions. We use  $d_{\tau s}^v(\mathbf{k})$  as the annihilation operator for tight-binding  $d$ -orbital states, and  $c_{\tau s}^n(\mathbf{k})$  for the eigenstates of the noninteracting Hamiltonian,  $\lambda_{\mathbf{k}}$  for the energy dispersion for Bogoliubov quasiparticles, and  $\Delta_{\mathbf{k}}$  for the superconducting gap function.

### A. Induced state

A proximity  $s$ -wave superconductor will inject Cooper pairs according to

$$H^V = \sum_{\mathbf{k}, \nu, \tau} B_{\nu}^* d_{\tau \downarrow}^{\nu}(-\mathbf{k}) d_{\tau \uparrow}^{\nu}(\mathbf{k}) + \frac{\varepsilon}{2} + \text{H.c.} \quad (5)$$

The coupling constants  $B_{\nu}$  and the overall constant  $\varepsilon$  depend on the material interface.<sup>1</sup> Using the abbreviated notation  $c_{\mathbf{k}\alpha} = c_{\tau s}^n(\mathbf{k})$ , with  $\alpha = \uparrow\downarrow$  for  $\tau = s = \pm$ , projecting onto the upper valence bands yields,

$$P_{\tau s}^{n=-} (H^0 + H^V - \mu N) = \sum_{\mathbf{k}, \alpha} \xi_{\mathbf{k}} c_{\mathbf{k}\alpha}^{\dagger} c_{\mathbf{k}\alpha} - \sum_{\mathbf{k}} (\Delta_{\mathbf{k}}^* c_{-\mathbf{k}\downarrow} c_{\mathbf{k}\uparrow} + \Delta_{\mathbf{k}} c_{\mathbf{k}\uparrow}^{\dagger} c_{-\mathbf{k}\downarrow}^{\dagger}) + \varepsilon, \quad (6)$$

where  $\xi_{\mathbf{k}} = E_{\tau \uparrow}^-(|\mathbf{k}|) - \mu$  and the effective BCS gap function is

$$\Delta_{\mathbf{k}} = \frac{1}{2}(B_+ + B_-) + \frac{1}{2}(B_+ - B_-) \cos \theta_{\mathbf{k}}, \quad (7)$$

with  $\theta_{\mathbf{k}} = \theta_{\tau \uparrow}^-(|\mathbf{k}|)$ . This form is identical to the standard BCS Hamiltonian with an effective spin index  $\alpha$ . However, the spin state of the Cooper pair is an equal superposition of the singlet and the  $m = 0$  component of spin triplet. The corresponding quasiparticle eigenstates are  $\gamma_{\mathbf{k}\alpha} = \alpha \cos \beta_{\mathbf{k}} c_{\mathbf{k}\alpha} + \sin \beta_{\mathbf{k}} c_{-\mathbf{k}, -\alpha}^{\dagger}$ , with energies  $\lambda_{\mathbf{k}} = \pm \sqrt{\xi_{\mathbf{k}}^2 + \Delta_{\mathbf{k}}^2}$ , where  $\cos 2\beta_{\mathbf{k}} = \xi_{\mathbf{k}}/\lambda_{\mathbf{k}}$ . Note that if  $B_+ = B_-$ , then  $\Delta_{\mathbf{k}}$  is a constant and independent of  $\mathbf{k}$ . Even when  $B_+$  and  $B_-$  are different, the constant term dominates. Before exploring the nature of this state, we analyze the case of intrinsic superconductivity, and show that the same state is energetically preferred.

<sup>1</sup>Note that all sums over  $\mathbf{k}$  are restricted to  $|\mathbf{k}|$  less than some cutoff that restricts the momentum to a single valley.

### B. Intrinsic phase

For a local attractive density-density interaction (e.g., one mediated by phonons), the potential is  $V \simeq \frac{1}{2} \sum_{\mathbf{R}, \mathbf{R}'} v_{\mathbf{R}\mathbf{R}'} : n_{\mathbf{R}} n_{\mathbf{R}'} :$ , with  $v_{\mathbf{R}\mathbf{R}'} = v_0 \delta_{\mathbf{R}\mathbf{R}'}$  and  $n_{\mathbf{R}}$  the total Wannier electron density at lattice vector  $\mathbf{R}$ . Projecting onto states near the chemical potential gives

$$P_{\tau=s}^{n=-} (H^V) = \sum_{\mathbf{k}, \mathbf{k}'} v(\mathbf{k}' - \mathbf{k}) \times (A_{\mathbf{k}\mathbf{k}'}^2 c_{\mathbf{k}'\uparrow}^\dagger c_{-\mathbf{k}'\uparrow}^\dagger c_{-\mathbf{k}\uparrow} c_{\mathbf{k}\uparrow} + A_{\mathbf{k}\mathbf{k}'}^2 c_{\mathbf{k}'\downarrow}^\dagger c_{-\mathbf{k}'\downarrow}^\dagger c_{-\mathbf{k}\downarrow} c_{\mathbf{k}\downarrow} + 2|A_{\mathbf{k}\mathbf{k}'}|^2 c_{\mathbf{k}'\uparrow}^\dagger c_{-\mathbf{k}'\downarrow}^\dagger c_{-\mathbf{k}\downarrow} c_{\mathbf{k}\uparrow}), \quad (8)$$

where

$$A_{\mathbf{k}\mathbf{k}'} = e^{i(\phi_{\mathbf{k}'} - \phi_{\mathbf{k}})} \sin \frac{\theta_{\mathbf{k}'}}{2} \sin \frac{\theta_{\mathbf{k}}}{2} + \cos \frac{\theta_{\mathbf{k}'}}{2} \cos \frac{\theta_{\mathbf{k}}}{2}. \quad (9)$$

The first two terms in Eq. (8) lead to intravalley pairing, and the third to intervalley pairing. We analyze the possible states within mean-field theory. The BCS order parameter is

$$\chi = v_0 \sum_{\mathbf{k}} g_{\mathbf{k}}^* \langle c_{-\mathbf{k}\alpha} c_{\mathbf{k}\alpha} \rangle, \quad (10)$$

where the form of  $g_{\mathbf{k}}$  depends on the particular pairing channel. The resulting Hamiltonian has the same form as the BCS Hamiltonian in Eq. (6) but with an effective  $\Delta_{\mathbf{k}} = g_{\mathbf{k}} \chi$ . The intravalley pairing has three symmetry channels, with the couplings given by  $2g_{\mathbf{k}} = 1 + \cos \theta_{\mathbf{k}}$ ,  $\sqrt{2}e^{-i\phi_{\mathbf{k}}} g_{\mathbf{k}} = \sin \theta_{\mathbf{k}}$  and  $2e^{-2i\phi_{\mathbf{k}}} g_{\mathbf{k}} = 1 - \cos \theta_{\mathbf{k}}$ . For these channels, since  $\langle c_{-\mathbf{k}\alpha} c_{\mathbf{k}\alpha} \rangle = -\langle c_{\mathbf{k}\alpha} c_{-\mathbf{k}\alpha} \rangle$ , relabeling  $\mathbf{k} \rightarrow -\mathbf{k}$  in the sum gives  $\chi = 0$ .<sup>2</sup> The intervalley pairing also has three symmetry channels:  $g_{\mathbf{k}} = \sqrt{2}$ ,  $g_{\mathbf{k}} = \sqrt{2} \cos \theta_{\mathbf{k}}$ , and  $g_{\mathbf{k}} = \sqrt{2} \sin \theta_{\mathbf{k}} \hat{\mathbf{k}}$ . Of the three, the constant valued channel is dominant.<sup>3</sup> This is to be expected, as the local density-density interaction leads to the largest pairing for electrons of opposite spins. Since the intravalley processes have the same spin, they are disfavored as compared to the intervalley pairing.

The key features of the intrinsic superconducting state are identical to the proximally induced case when density-density interactions dominate. We restrict further analysis to that case, and turn to the question of pair-breaking phenomena induced either by optical or magnetic fields.

### IV. OPTOELECTRONIC COUPLING

The noninteracting system displays valley selective optical excitations. Light of a particular polarization only couples to one valley. Since the superconducting state is a coherent condensate admixing the two valleys, we address whether pair-breaking displays similar valley selectivity. In particular, we explore whether or not the two quasiparticles generated by circularly polarized light, with total energy larger than

<sup>2</sup>For odd parity interactions, where  $v(-\mathbf{k}) = -v(\mathbf{k})$ , the intravalley pairing is not excluded by symmetry. Specifically, repeating the calculation with this assumption, the intervalley terms fully cancel, and one obtains Eq. (8) without the intervalley term on the third line.

<sup>3</sup>For example, using the values for WSe<sub>2</sub>,  $\sin^2 \theta_{\mathbf{k}} = 0.44$  and  $\cos^2 \theta_{\mathbf{k}} = 0.56$  at the chemical potential.

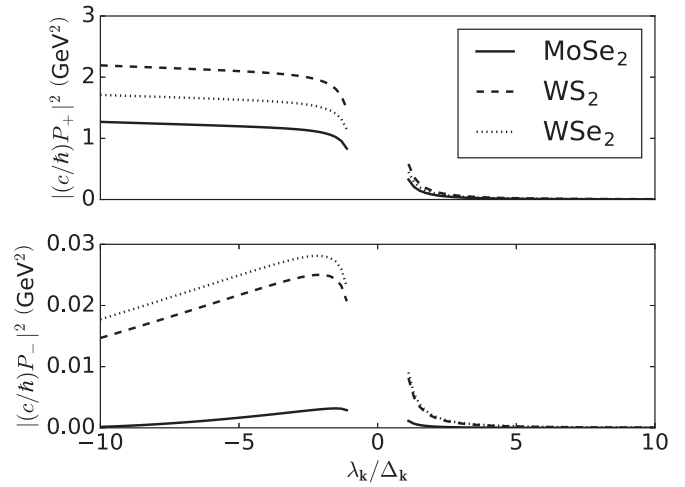


FIG. 2. Optical transition rate matrix elements  $|P_{\pm}|^2$  in the superconducting phase as a function of the ratio of the quasiparticle energy  $\lambda_{\mathbf{k}}$  to the superconducting gap  $\Delta_{\mathbf{k}}$ . Material parameters for MoSe<sub>2</sub>, WS<sub>2</sub>, and WSe<sub>2</sub> are given in Ref. [26] and a gap of  $\Delta_{\mathbf{k}} = 7.5$  meV is chosen for illustrative purposes. The order-of-magnitude contrast between  $|P_{+}|^2$  and  $|P_{-}|^2$  causes the optical-valley selectivity.

$E_g + \Delta_{\mathbf{k}}$ , occupy opposite valleys, with one in the conduction band and the other in the valence band.

The optical excitations arise from the Berry curvature, which acts as an effective angular momentum. The electromagnetic potential  $\mathbf{A}$ , with polarization vector  $\boldsymbol{\epsilon}$ , is introduced using minimal coupling,  $H_{\tau s}^{v v'}(\mathbf{k}) \rightarrow H_{\tau s}^{v v'}(\mathbf{k} + e\mathbf{A})$ , where, in the dipole approximation,  $\mathbf{A} = 2 \text{Re} \epsilon A_0 e^{-i\omega t}$ . This yields a perturbed Hamiltonian  $H \rightarrow H + H^A$ , where  $H^A = H' e^{-i\omega t} + H'^{\dagger} e^{i\omega t}$ , with

$$H' = \sum_{\mathbf{k}, \tau, s} H'_{\tau} d_{\tau s}^{-\dagger}(\mathbf{k}) d_{\tau s}^{+}(\mathbf{k}) - \sum_{\mathbf{k}, \tau, s} H'_{-\tau} d_{\tau s}^{+\dagger}(\mathbf{k}) d_{\tau s}^{-}(\mathbf{k}), \quad (11)$$

and  $H'_{\tau} = ateA_0(\tau \hat{\mathbf{x}} + i\hat{\mathbf{y}}) \cdot \boldsymbol{\epsilon}$ . The transition rate is proportional to the modulus-squared of the optical matrix elements,  $\mathbf{P}_{\tau s}^{n n'}(\mathbf{k})$ , defined by

$$H^A = \sum_{\substack{\mathbf{k}, \tau, s \\ n, n'}} \frac{eA_0}{m_0} \boldsymbol{\epsilon} \cdot \mathbf{P}_{\tau s}^{n n'}(\mathbf{k}) c_{\tau s}^{n \dagger}(\mathbf{k}) c_{\tau s}^{n'}(\mathbf{k}). \quad (12)$$

For circularly polarized light, in the absence of superconductivity,  $\boldsymbol{\epsilon}_{\pm} = (\hat{\mathbf{x}} \pm i\hat{\mathbf{y}})/\sqrt{2}$  and

$$\boldsymbol{\epsilon}_{\pm} \cdot \mathbf{P}_{\tau s}^{+-}(\mathbf{k}) = \mp \tau \sqrt{2} a t m_0 e^{\pm i\phi} \sin^2 \frac{\theta_{\tau s}^{\mp \tau}(k)}{2}. \quad (13)$$

The transition rate matrix elements for optical excitations from the BCS ground state are given by Eq. (13) multiplied by a coherence factor  $\sin \beta_{\mathbf{k}}$ . Since  $\theta_{\tau s}^{-}(k) - \theta_{\tau s}^{+}(k) = \tau\pi$ , switching either the valley or polarization transforms  $\sin \rightarrow \cos$  in Eq. (13), giving matrix elements  $|P_{\pm}| = |\boldsymbol{\epsilon}_{\pm} \cdot \mathbf{P}_{\tau s}^{\pm \pm}(\mathbf{k}) \sin \beta_{\mathbf{k}}|$  corresponding to matching ( $P_{+}$ ) or mismatching ( $P_{-}$ ) polarization-valley indexes. For a given valley, a chosen polarization of light couples more strongly than the other, as is evident comparing  $|P_{+}|^2$  to  $|P_{-}|^2$  and shown in Fig. 2. For incident light with energy  $E_g + |\lambda_{\mathbf{k}}|$ , right circularly polarized light (+) has a higher probability

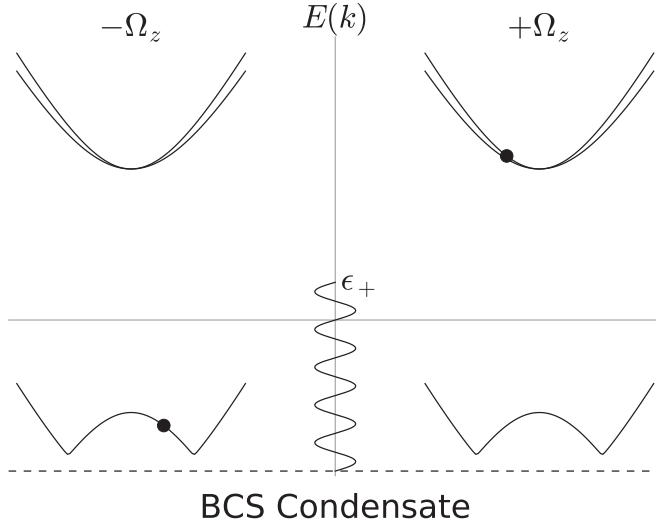


FIG. 3. Pair-breaking by right circularly polarized light leads to an electron in the conduction band of the right valley and a partner in the valence band of the left valley. The valleys interchange for left circularly polarized light.

of promoting a quasiparticle to the right conduction band, as reflected in the larger matrix element  $|P_+|^2 \gg |P_-|^2$ . As depicted in Fig. 3, the partner of the Cooper pair is in the valence band in the opposite valley. The other valley has the opposite dependence on polarization.

This key new result opens the door for valley control of excitations from a coherent ground state. For example, the two quasiparticles have the same charge and Berry curvature (see below). In the presence of an electric field, they both acquire the same transverse anomalous velocity. Thus, in contrast to the response in the normal state, an anomalous Hall effect is anticipated with no accompanying spin current.

### V. BERRY CURVATURE

The Berry curvature in the noninteracting crystal for left and right circularly polarized ( $\epsilon_{\pm}$ ) optical excitations for a given  $\mathbf{k}$  is  $\pm 2\Omega_{\pm}^+(k)$ , where

$$\Omega_{\tau s}^n(k) = \hat{\mathbf{z}} \cdot \Omega_{\tau s}^n(\mathbf{k}), \quad (14a)$$

$$= -n\tau \left[ \frac{1}{2k} \frac{\partial}{\partial k} \theta_{\tau s}^n(k) \right] \sin \theta_{\tau s}^n(k), \quad (14b)$$

$$= -n\tau \frac{2(at)^2 (E_g - \tau s E_{\text{soc}})}{[(2atk)^2 + (E_g - \tau s E_{\text{soc}})^2]^{3/2}}. \quad (14c)$$

The BCS ground state<sup>4</sup> is

$$|\Omega\rangle = \prod_{\mathbf{k}} \text{csc } \beta_{\mathbf{k}} \gamma_{\mathbf{k}\uparrow} \gamma_{-\mathbf{k}\downarrow} |0\rangle, \quad (15a)$$

$$= \prod_{\mathbf{k}} (\cos \beta_{\mathbf{k}} - \sin \beta_{\mathbf{k}} c_{\mathbf{k}\uparrow}^{\dagger} c_{-\mathbf{k}\downarrow}^{\dagger}) |0\rangle. \quad (15b)$$

<sup>4</sup>Note that the full ground state also contains the two lower filled bands, but those contribute zero net Berry curvature and may be ignored in this section and the next.

This superconducting state is built up from the quasiparticle eigenstates,  $|\mathbf{k}\rangle = \text{csc } \beta_{\mathbf{k}} \gamma_{\mathbf{k}\uparrow} \gamma_{-\mathbf{k}\downarrow} |0\rangle$ , of the  $\mathbf{k}$ -dependent Hamiltonian  $\lambda_{\mathbf{k}}(\gamma_{\mathbf{k}\uparrow}^{\dagger} \gamma_{\mathbf{k}\uparrow} + \gamma_{-\mathbf{k}\downarrow}^{\dagger} \gamma_{-\mathbf{k}\downarrow})$ . The  $z$  component of the Berry curvature of the correlated state is zero,

$$\hat{\mathbf{z}} \cdot i \nabla_{\mathbf{k}} \times \langle \mathbf{k} | \nabla_{\mathbf{k}} | \mathbf{k} \rangle = \Omega_{+\uparrow}^-(k) + \Omega_{-\downarrow}^-(k) = 0. \quad (16)$$

A single optically excited state in the left valley for a given  $\mathbf{k}$  is  $c_{+\uparrow}^{\dagger}(\mathbf{k}) c_{+\uparrow}^-(\mathbf{k}) |0\rangle$ , which has a Berry curvature  $+2 \sin^6 \beta_{\mathbf{k}} \Omega_{+\uparrow}^+(k)$ . The corresponding excitation in the right valley has a Berry curvature of the same magnitude but opposite sign.

### VI. IN-PLANE MAGNETIC FIELD AND SCALAR DISORDER

In this section, we discuss the effects of in-plane magnetic fields and nonmagnetic impurities on the superconducting state. We consider the lightly hole-doped monolayer TMDs in the regime where the Fermi level crosses the upper valence bands and is well separated from the lower valence bands. In this regime, the system is a spin-valley locking system with the spin-opposite Fermi pocket at each valley. Without loss of generality, we adopt a simplified model taking into account the valence bands only. In a quasi-two-dimensional (2D) system, an in-plane magnetic field couples to quasiparticles through spin paramagnetism with negligible orbital interactions. Applying a uniform in-plane magnetic field in the  $x$  direction  $\mathbf{B} = (B, 0, 0)$ , the system is described by the Hamiltonian ( $\hbar = k_B = c = 1$ )

$$\mathcal{H}_{\tau}(\mathbf{k}) = -\frac{k^2}{2m} - \mu + \tau E_{\text{soc}} \hat{s}_z + \mu_B B \hat{s}_x, \quad (17)$$

which is acting on the valley-spin basis  $\phi_{\tau}(\mathbf{k}) = (c_{\tau\uparrow}(\mathbf{k}), c_{\tau\downarrow}(\mathbf{k}))^T$ , where  $\mu$  is the chemical potential,  $\tau = \pm$  is the valley index,  $\hat{s}_i$  are Pauli matrices operating in spin space, and  $\mu_B$  is the Bohr magneton. The dispersion relations of the upper and lower valence bands have been approximated by a quadratic form with an effective mass  $m = E_g / (2a^2 t^2)$ , where  $E_g$  is the large energy gap between the conduction and valence bands,  $E_g \gg E_{\text{soc}}$ ,  $a$  and  $t$  are defined under Eq. (1), and the momentum  $\mathbf{k} = (k_x, k_y)$  is measured from the corresponding valley center with  $k = |\mathbf{k}|$ . Note that in this section we use  $\mathbf{k}$  to represent momentum measured from the corresponding valley center and  $\mathbf{p}$  to represent momentum measured from the Brillouin zone (BZ) center. We use the notation that  $c_{\tau s}^{\dagger}(\mathbf{k})$  ( $c_{\tau s}(\mathbf{k})$ ) creates (annihilates) a quasiparticle with momentum  $\mathbf{k}$  and spin  $s$  in the valley  $\tau$ , and  $c_s^{\dagger}(\mathbf{p})$  ( $c_s(\mathbf{p})$ ) creates (annihilates) a quasiparticle with momentum  $\mathbf{p}$  and spin  $s$ .

The Hamiltonian  $\mathcal{H}_{\tau}(\mathbf{k})$  has the spectrum

$$E_{\tau, u/l}(k) = -\frac{k^2}{2m} - \mu \pm \sqrt{E_{\text{soc}}^2 + (\mu_B B)^2}, \quad (18)$$

with  $u$  for the upper (+) and  $l$  for the lower (-) band at each valley, and the eigenstates  $\varphi_{\tau}(\mathbf{k}) = (c_{\tau u}(\mathbf{k}), c_{\tau l}(\mathbf{k}))^T$ , where  $c_{\tau u}$  and  $c_{\tau l}$  correspond to the quasiparticles in the band basis which is related to the spin basis through a field and valley-dependent unitary transformation  $U_{\tau}(b)$ :  $\varphi_{\tau}(\mathbf{k}) = U_{\tau}(b) \phi_{\tau}(\mathbf{k})$ , where  $b = \mu_B B / E_{\text{soc}}$  is the dimensionless magnetic field. Applying a uniform in-plane magnetic field shifts both the upper (lower) valence bands at the two valleys by the same amount

(but the opposite amount between the upper and lower band at each valley), so that the perfect nesting condition between the Fermi pockets at the two valleys remains. Meanwhile, the quasiparticle spin acquires a finite in-plane component, i.e., deviating from  $\pm z$  direction. Explicitly, we have  $\langle \tau, u | \hat{s}_z | \tau, u \rangle = -\langle \tau, l | \hat{s}_z | \tau, l \rangle = (\tau/2)/\sqrt{1+b^2}$ , and  $\langle \tau, u | \hat{s}_x | \tau, u \rangle = -\langle \tau, l | \hat{s}_x | \tau, l \rangle = (b/2)/\sqrt{1+b^2}$ . Therefore, at both valleys, the quasiparticle spin tilts towards the field direction in the upper valence bands and tilts against the field direction in the lower valence bands. The change of quasiparticle spin orientation induced by the in-plane field modifies the internal structure of the Cooper pair and affects the pairing strength as shown below.

To evaluate the effect of the magnetic field on the superconductivity, we follow the procedure used in Sec. III. A local attractive density-density interaction with pairing strength  $v_0$  can be written as:  $\mathcal{H}_{\text{int}} = -v_0 \int d^2\mathbf{r} \rho(\mathbf{r}) \rho(\mathbf{r})$  with the quasiparticle density  $\rho(\mathbf{r}) = \sum_s c_s^\dagger(\mathbf{r}) c_s(\mathbf{r})$ , where  $c_s^\dagger(\mathbf{r})$  ( $c_s(\mathbf{r})$ ) is the Fourier transform of  $c_s^\dagger(\mathbf{p})$  ( $c_s(\mathbf{p})$ ). Transforming to momentum space and projecting onto the upper valence bands, the pairing Hamiltonian has the form

$$\mathcal{H}_p = -v'(b) \sum_{\mathbf{k}, \mathbf{k}'} c_+^\dagger(\mathbf{k}) c_-^\dagger(-\mathbf{k}) c_-(-\mathbf{k}') c_+(\mathbf{k}'), \quad (19)$$

where we have ignored the upper-band subscript  $u$  in the operators  $c_{\tau u}^\dagger$  and  $c_{\tau u}$ . The effective pairing strength in the presence of in-plane magnetic field is  $v'(b) = v_0/(1+b^2)$ . The Hamiltonian  $\mathcal{H}_p$  describes an intervalley pairing with a pairing strength  $v'$  suppressed by the in-plane field. At zero field,  $v' = v_0$ ,  $c_+^\dagger = c_{+\uparrow}^\dagger$ , and  $c_-^\dagger = c_{-\downarrow}^\dagger$ , so the pairing occurs between opposite spins. At finite fields,  $v' < v_0$  and the quasiparticle at valley  $+$  ( $-$ ), represented by  $c_+^\dagger$  ( $c_-^\dagger$ ), has its up (down) spin tilted towards the field direction. As a result, the intervalley pairing contains equal-spin pairing components in the presence of in-plane field.

The mean-field Hamiltonian, using the Nambu-valley basis  $\Psi_{\mathbf{k}} = (c_+(\mathbf{k}), c_-(\mathbf{k}), c_-^\dagger(-\mathbf{k}), -c_+^\dagger(-\mathbf{k}))^T$ , takes the form

$$\mathcal{H}_{\text{MF}}(\mathbf{k}) = \xi_{\mathbf{k}} \hat{\eta}_z - \Delta \hat{\eta}_x, \quad (20)$$

where  $\hat{\eta}_i$  are Pauli matrices acting on Nambu (particle-hole) space,  $\xi_{\mathbf{k}} = -k^2/2m - \mu + \sqrt{E_{\text{soc}}^2 + (\mu_B B)^2}$ , and the mean field  $\Delta = v'(b) \sum_{\mathbf{k}'} \langle c_-(-\mathbf{k}') c_+(\mathbf{k}') \rangle$  describes an intervalley pairing field, which we choose to be real for convenience.

In a conventional 2D superconductor with a spin-degenerate Fermi surface, the application of an in-plane magnetic field induces an energy splitting between opposite-spin bands. This energy mismatch between opposite spins creates a pair-breaking effect in the clean system characterized by the pair-breaking equation for temperature  $T \leq T_c^0$  [35],

$$\ln \frac{T_c^0}{T} = \frac{1}{2} \left[ \psi \left( \frac{1}{2} + \frac{i\mu_B B_c}{2\pi T} \right) + \psi \left( \frac{1}{2} - \frac{i\mu_B B_c}{2\pi T} \right) \right] - \psi \left( \frac{1}{2} \right), \quad (21)$$

where  $T_c^0$  is the transition temperature at zero field in the clean system and  $\psi(z)$  is the digamma function. This equation determines the critical field  $B_c$  that destroys the supercon-

ducting state at temperature  $T \leq T_c^0$  from spin paramagnetism. Furthermore, the scattering from nonmagnetic impurities does not alter this pair-breaking Eq. (21) such that the critical field remains the same regardless of the presence of scalar disorders [35].

Unlike the conventional 2D superconductors, in our system the two single-spin Fermi pockets at different valleys remain perfectly nested without the energy mismatch caused by spin paramagnetism, and the spins at the two pockets are no longer opposite with equal-spin components induced by the field. These two differences give rise to new features in the spin-valley locking system from the effects of in-plane magnetic fields. First, in the clean limit, the presence of in-plane magnetic fields does not lead to a pair-breaking effect for the lack of energy mismatch, but mildly suppresses the transition temperature through the weakening of the pairing strength. The suppressed transition temperature  $T_c'$  is related to the zero-field transition temperature  $T_c^0$  as  $T_c' = T_c^0 \exp(-b^2/v_0 N_F)$  in the mean-field theory, where  $N_F$  is the density of states at the Fermi level. Second, the superconducting state is no longer immune to the scalar disorder, since nonmagnetic disorder potential can cause intervalley scattering due to the field-induced parallel-spin components on the two pockets. This interplay between the in-plane magnetic field and the scalar disorder leads to a pair-breaking effect.

In the presence of dilute randomly distributed nonmagnetic impurities, the Hamiltonian for short-range impurity potential is given by

$$\mathcal{H}_{\text{imp}} = \sum_j \int d^2\mathbf{r} U_0 \delta(\mathbf{r} - \mathbf{R}_j) \rho(\mathbf{r}), \quad (22)$$

where  $\mathbf{R}_j$  is the position of the  $j$ th impurity and  $U_0$  is the disorder strength. Transforming to momentum space and projecting onto the upper valence bands,  $\mathcal{H}_{\text{imp}}$  can be written using the Nambu-valley basis  $\Psi_{\mathbf{k}}$  as

$$\mathcal{H}_{\text{imp}} = \sum_{\mathbf{k}_1, \mathbf{k}_2} \sum_j e^{i(\mathbf{k}_1 - \mathbf{k}_2) \cdot \mathbf{R}_j} \Psi_{\mathbf{k}_1}^\dagger \hat{U} \Psi_{\mathbf{k}_2}, \quad (23)$$

with the disorder scattering vertex  $\hat{U}$  taking the form

$$\hat{U} = U_0 \hat{\eta}_z + U_0 \frac{b}{\sqrt{1+b^2}} \hat{\tau}_x, \quad (24)$$

where  $\hat{\tau}_i$  are Pauli matrices operating in valley space. The first term in  $\hat{U}$  corresponds to intravalley scattering and the second term corresponds to intervalley scattering. Note that we have ignored the factors  $e^{i(\pm 2\mathbf{K}) \cdot \mathbf{R}_j}$  in the intervalley terms because  $e^{i(2\mathbf{K}) \cdot \mathbf{R}_j}$  and  $e^{i(-2\mathbf{K}) \cdot \mathbf{R}_j}$  will appear in pair and cancel each other in the diagrammatical calculation of self energy.

The self-energy due to impurity scattering after averaging over randomly distributed impurity configurations, in the first-order Born approximation, is obtained as [36,37]

$$\hat{\Sigma}(\mathbf{k}, i\omega_n) = n_{\text{imp}} \int \frac{d^2\mathbf{k}'}{(2\pi)^2} \hat{U} \hat{\mathcal{G}}_0(\mathbf{k}', i\omega_n) \hat{U}, \quad (25)$$

where  $n_{\text{imp}}$  is the impurity concentration and  $\hat{\mathcal{G}}_0$  is the Green's function matrix of the clean system,  $\hat{\mathcal{G}}_0(\mathbf{k}', i\omega_n) = (i\omega_n - \xi_{\mathbf{k}'} \hat{\eta}_z + \Delta \hat{\eta}_x)^{-1}$ , with the Matsubara frequencies  $\omega_n = (2n+1)\pi T$ . After integrating out  $\xi$  in the self-energy, the

disorder renormalized Green's function matrix  $\hat{G} = (\hat{G}_0^{-1} - \hat{\Sigma})^{-1}$  can be parameterized as

$$\hat{G}(\mathbf{k}, i\omega_n) = [i\tilde{\omega}_n - \xi_{\mathbf{k}}\hat{\eta}_z + \tilde{\Delta}\hat{\eta}_x + iF(\omega_n)\hat{\eta}_z\hat{\tau}_x]^{-1}, \quad (26)$$

where the quantities  $\tilde{\omega}_n$ ,  $\tilde{\Delta}$ , and  $F(\omega_n)$  have the definitions

$$\tilde{\omega}_n = \omega_n + \left(\frac{1}{2\tau_1} + \frac{1}{2\tau_2}\right) \frac{\omega_n}{\sqrt{\omega_n^2 + \Delta^2}}, \quad (27)$$

$$\tilde{\Delta} = \Delta + \left(\frac{1}{2\tau_1} - \frac{1}{2\tau_2}\right) \frac{\Delta}{\sqrt{\omega_n^2 + \Delta^2}}, \quad (28)$$

$$F(\omega_n) = \frac{1}{2\tau_1} \frac{\omega_n}{\sqrt{\omega_n^2 + \Delta^2}} \frac{2b}{\sqrt{1+b^2}}. \quad (29)$$

Here,  $1/\tau_1$  and  $1/\tau_2$  are the collision rates corresponding to the disorder-induced intravalley and intervalley scattering, respectively, with the expressions

$$\frac{1}{\tau_1} = 2U_0^2 n_{\text{imp}} \pi N_F, \quad \frac{1}{\tau_2} = \frac{1}{\tau_1} \frac{b^2}{1+b^2}. \quad (30)$$

In the superconducting state, the self-consistency equation for the order parameter is given by

$$\Delta = \frac{1}{4} v' T \sum_n \int \frac{d^2\mathbf{k}}{(2\pi)^2} \text{Tr}[\hat{\eta}_x \hat{G}(\mathbf{k}, i\omega_n)], \quad (31)$$

where  $\text{Tr}[\dots]$  is the trace of the argument. Explicitly, from Eq. (26), it has the form

$$\Delta = v' \pi N_F T \sum_n \frac{\tilde{\Delta}}{\sqrt{\tilde{\omega}_n^2 + \tilde{\Delta}^2}}. \quad (32)$$

Linearizing the self-consistency Eq. (32) near the critical field  $B_c$ , we obtain the pair-breaking equation due to the interplay between the in-plane field and the scalar disorder,

$$\ln \frac{T'(b_c)}{T} = \psi\left(\frac{1}{2} + \frac{\delta_c}{2\pi T}\right) - \psi\left(\frac{1}{2}\right), \quad (33)$$

where  $T'_c(b_c) = T_c^0 \exp(-b_c^2/v_0 N_F)$  is the transition temperature in the clean system in the presence of the field  $b_c = \mu_B B_c/E_{\text{soc}}$ , and the pair-breaking parameter

$$\delta_c = \frac{1}{\tau_2} \Big|_{b_c} = \frac{1}{\tau_1} \frac{b_c^2}{1+b_c^2} \quad (34)$$

arises from the valley-flip scattering process. Equation (33) determines the in-plane critical field  $B_c(T)$  at temperature

$T \leq T'_c$ . For  $b_c \ll 1$ , the pair-breaking parameter takes the simple form  $\delta_c \approx \tau_1^{-1} (\mu_B B_c/E_{\text{soc}})^2$ .

As  $T \rightarrow 0$ , the pair-breaking Eq. (33) can be approximated by the asymptotic expansion of the digamma function, which leads to  $2\pi T'_c \exp[\psi(1/2)] = (b_c^2/\tau_1)/(1+b_c^2)$ . At finite disorder concentration,  $\tau_1^{-1} \neq 0$ , when  $b_c \ll 1$  with  $T'_c \approx T_c^0$ , the critical field at zero temperature is approximated as

$$\mu_B B_c \Big|_{T \rightarrow 0} \approx E_{\text{soc}} [2\pi e^{\psi(1/2)} k_B T_c^0 \tau_1/\hbar]^{1/2}, \quad (35)$$

where we have put back the Boltzmann constant  $k_B$  and the reduced Planck constant  $\hbar$ . The large spin-orbit interaction  $E_{\text{soc}}$  ( $\sim 150-500$  meV) in monolayer TMDs indicates that the in-plane critical field  $B_c$  is significantly enhanced, well beyond the Pauli limit.

## VII. CONCLUSIONS

In this letter, we report on the nature of the superconducting state of hole-doped TMDs. Remarkably, the correlated state inherits the valley contrasting phenomena of the noninteracting state. While the magnitude is smaller, pair-breaking produces quasiparticles that have the same Berry curvature, and hence the same anomalous velocity. Thus one predicts an anomalous Hall response unlike the valley Hall response observed in  $\text{MoSe}_2$ .

Spin-valley locking leads to large critical magnetic fields. A similar phenomenon was recently reported in heavily hole-doped (beyond the spin-split gap)  $\text{NbSe}_2$  [29]. In the new regime, where only one band per valley intersects the chemical potential, no pair-breaking occurs for in-plane fields unless disorder is present. While systematic synthesis and characterization of hole-doped systems is still in its early stages, the fact that other two-dimensional compounds and their bulk counterparts are known to be superconducting [38] provides impetus to explore this novel phenomena.

## ACKNOWLEDGMENTS

The software developed [39] and used [40] for this work and the included figures is available freely online. We thank Michael Phillips for useful discussions. We acknowledge the support of the Army Research Office through Grant ARO W911NF1510079.

[1] F. D. M. Haldane, *Phys. Rev. Lett.* **61**, 2015 (1988).  
 [2] C. L. Kane and E. J. Mele, *Phys. Rev. Lett.* **95**, 226801 (2005).  
 [3] B. A. Bernevig and S.-C. Zhang, *Phys. Rev. Lett.* **96**, 106802 (2006).  
 [4] M. König, S. Wiedmann, C. Brüne, A. Roth, H. Buhmann, L. W. Molenkamp, X.-L. Qi, and S.-C. Zhang, *Science* **318**, 766 (2007).  
 [5] M. Z. Hasan and C. L. Kane, *Rev. Mod. Phys.* **82**, 3045 (2010).  
 [6] X.-L. Qi and S.-C. Zhang, *Rev. Mod. Phys.* **83**, 1057 (2011).  
 [7] W. Witczak-Krempa, G. Chen, Y. B. Kim, and L. Balents, *Annu. Rev. Condens. Matter Phys.* **5**, 57 (2014).

[8] B. Radisavljevic, A. Radenovic, J. Brivio, V. Giacometti, and A. Kis, *Nat. Nanotechnol.* **6**, 147 (2011).  
 [9] Z. Y. Zhu, Y. C. Cheng, and U. Schwingenschlögl, *Phys. Rev. B* **84**, 153402 (2011).  
 [10] Y. Zhang, J. Ye, Y. Matsushashi, and Y. Iwasa, *Nano Lett.* **12**, 1136 (2012).  
 [11] Q. H. Wang, K. Kalantar-Zadeh, A. Kis, J. N. Coleman, and M. S. Strano, *Nat. Nanotechnol.* **7**, 699 (2012).  
 [12] J. T. Ye, Y. J. Zhang, R. Akashi, M. S. Bahrmy, R. Arita, and Y. Iwasa, *Science* **338**, 1193 (2012).  
 [13] W. Bao, X. Cai, D. Kim, K. Sridhara, and M. S. Fuhrer, *Appl. Phys. Lett.* **102**, 042104 (2013).

- [14] F. Zahid, L. Liu, Y. Zhu, J. Wang, and H. Guo, *AIP Adv.* **3**, 052111 (2013),
- [15] E. Cappelluti, R. Roldán, J. A. Silva-Guillén, P. Ordejón, and F. Guinea, *Phys. Rev. B* **88**, 075409 (2013).
- [16] X. Xu, W. Yao, D. Xiao, and T. F. Heinz, *Nat. Phys.* **10**, 343 (2014).
- [17] T. Das and K. Dolui, *Phys. Rev. B* **91**, 094510 (2015).
- [18] J. Lee, K. F. Mak, and J. Shan, [arXiv:1508.03068](https://arxiv.org/abs/1508.03068) [cond-mat.mes-hall].
- [19] R. A. Bromley, R. B. Murray, and A. D. Yoffe, *J. Phys. C* **5**, 759 (1972).
- [20] T. Böker, R. Severin, A. Müller, C. Janowitz, R. Manzke, D. Voß, P. Krüger, A. Mazur, and J. Pollmann, *Phys. Rev. B* **64**, 235305 (2001).
- [21] K. F. Mak, C. Lee, J. Hone, J. Shan, and T. F. Heinz, *Phys. Rev. Lett.* **105**, 136805 (2010).
- [22] A. Splendiani, L. Sun, Y. Zhang, T. Li, J. Kim, C.-Y. Chim, G. Galli, and F. Wang, *Nano Lett.* **10**, 1271 (2010).
- [23] A. Kormányos, V. Zólyomi, N. D. Drummond, P. Rakyta, G. Burkard, and V. I. Fal'ko, *Phys. Rev. B* **88**, 045416 (2013).
- [24] G.-B. Liu, W.-Y. Shan, Y. Yao, W. Yao, and D. Xiao, *Phys. Rev. B* **88**, 085433 (2013).
- [25] D. Xiao, M.-C. Chang, and Q. Niu, *Rev. Mod. Phys.* **82**, 1959 (2010).
- [26] D. Xiao, G.-B. Liu, W. Feng, X. Xu, and W. Yao, *Phys. Rev. Lett.* **108**, 196802 (2012).
- [27] K. F. Mak, K. L. McGill, J. Park, and P. L. McEuen, *Science* **344**, 1489 (2014).
- [28] J. M. Lu, O. Zheliuk, I. Leermakers, N. F. Q. Yuan, U. Zeitler, K. T. Law, and J. T. Ye, *Science* **350**, 1353 (2015).
- [29] X. Xi, Z. Wang, W. Zhao, J.-H. Park, K. T. Law, H. Berger, L. Forro, J. Shan, and K. F. Mak, *Nat. Phys.* **12**, 139 (2016).
- [30] Y. Saito, Y. Nakamura, M. S. Bahrmy, Y. Kohama, J. Ye, Y. Kasahara, Y. Nakagawa, M. Onga, M. Tokunaga, T. Nojima, Y. Yanase, and Y. Iwasa, *Nat. Phys.* **12**, 144 (2016).
- [31] B. T. Zhou, N. F. Q. Yuan, H.-L. Jiang, and K. T. Law, *Phys. Rev. B* **93**, 180501 (2016).
- [32] N. F. Q. Yuan, K. F. Mak, and K. T. Law, *Phys. Rev. Lett.* **113**, 097001 (2014).
- [33] J. Zhang and V. Aji, *Phys. Rev. B* **94**, 060501 (2016).
- [34] L. P. Gor'kov and E. I. Rashba, *Phys. Rev. Lett.* **87**, 037004 (2001).
- [35] K. Maki and T. Tsuneto, *Prog. Theor. Phys.* **31**, 945 (1964).
- [36] A. A. Abrikosov and L. P. Gor'kov, *Sov. Phys. JETP* **12**, 1243 (1961).
- [37] K. Maki, in *Superconductivity*, edited by R. D. Parks (Dekker, New York, 1969).
- [38] R. Roldán, E. Cappelluti, and F. Guinea, *Phys. Rev. B* **88**, 054515 (2013).
- [39] Related software and source code at <https://evansosenko.com/dichalcogenides>.
- [40] J. D. Hunter, *Comput. Sci. Eng.* **9**, 90 (2007).